PSM
Biological Research

Research Article 2022 | Volume 7 | Issue 1 | 14-33

Open Access

Article Information

Received: November 19, 2021

Accepted: December 28, 2021

Online first: January 11. 2022

Published: January 22. 2022

Keywords

In vitro,
Callus culture,
Density functional theory,
Synthesized chromone glycosides.

Authors' Contribution

HHM conceived and designed the study. AMTA performed the experiments. AMTA and SAR analyzed data, wrote and revised the paper.

How to cite

Taj Al-Deen, A.M., Manaf, H.H., Rizk, S.A., 2022. HPLC of *Hypericum perforatum* Herb Cell Suspension Reveals Attractive Medical Flavanone Glycosides Compounds that are Supported by DFT Study. PSM Biol. Res., 7(1): 14-33.

***Correspondence**

Aziza M. Taj Aldeen
Email:
azizataj1@yahoo.com

HPLC of *Hypericum perforatum* Herb Cell Suspension Reveals Attractive Medical Flavanone Glycosides Compounds that are Supported by DFT Study

Aziza M. Taj Al-Deen[1]*, Hossam H. Manaf[2], Sameh A. Rizk[3]

[1]Biology Department, Faculty of Science, Sana'a University, Sana'a, Yemen.
[2]Agricultural Botany Department, Faculty of Agriculture, Ain Shams University, Cairo, Egypt.
[3]Chemistry Department, Faculty of Science, Ain Shams University, Cairo, Egypt.

Abstract:

In the present study, *in vitro Hypericum perforatum* leaves were used as a segment to induce callus culture. Callus morphogenesis was achieved using Murashige and Skoog's culture media supplemented with different combinations of growth regulators. The best callus biomass was obtained with 0.22 mg/l (2,4-D) + 0.024 mg/l (Kin), and cell suspension culture succeeded in the production of new good circular cell biomass that was treated by three different stimulating compounds. The results showed that the best increase in the active ingredients was by chromone glycoside derivatives 2-5, as revealed via HPLC test of fractionation. The extracted *H. perforatum* L. was conveniently synthesized in 3 steps, from the commercially available Acetophloroglucine, which supported the extracted ingredients 2-5. The glucosyl moiety was introduced by stereoselective O-glycosylation with a per-O-benzylated glucosyl bromide donor, followed by the formation of the chalcone with debenzylation, which was carried out to afford 3 and 5 with overall yields of 64% and 73%, respectively. Finally, the density functional theory (DFT) was then applied to explore the structural and electronic characteristics of these materials. All the synthesized compounds have been characterized based on their ^{1}H NMR, MS, and elemental analyses for the optimized precursors of the synthesized chromone glycosides.

INTRODUCTION

Oxidative stress plays an important role in the pathogenesis of cardiovascular diseases, mainly through oxidative modification of low-density lipoprotein (LDL) which initiates vascular inflammation and atherosclerotic lesion formation. Therefore, they have great potential to delay LDL oxidation with their radical scavenging activity and prevent cardiovascular disease (Hirano *et al.*, 2001; Sánchez-Moreno *et al.*, 2003; Steinberg, 1989). Flavonoids found in many vegetables and fruits are associated with a decreased risk of cardiovascular disease, display a strong antimicrobial and radical scavenging activity to be associated with reduced danger for certain chronic diseases, the prevention of some cardiovascular sicknesses, and certain types of cancerous processes (Al-Mahweety, 2016; Asres *et al.*, 2005; Gross, 2004; Knekt *et al.*, 2002; Kris-Etherton *et al.*, 2004; Nichenametla *et al.*, 2006). Flavonoids and other compounds found in plants show antiviral (Cushnie and Lamb, 2005), antimicrobial (Ali *et al.*, 2017; Hussain *et al.*, 2016; Iqbal and Ashraf, 2019; Kalim *et al.*, 2016; Kim *et al.*, 2004), antioxidant (Amin and Edris, 2017), anti-inflammatory activities (Bito *et al.*, 2002), helpful on capillary fragility (Benavente-García *et al.*, 1997), prevent human platelet aggregation (Tijburg *et al.*, 1997), antiulcer (Wightman, 2003), and antiallergenic (Middleton and Kandaswami, 1992).

However, the actual *in vivo* mechanism of action is largely unknown. Most studies have attentive *in vitro* tests at amounts much higher than in humans, however, few clinical investigations have been carried out around some diseases (Scalbert *et al.*, 2005). The possible mechanisms of potential experimental action have been studied (Nijveldt *et al.*, 2001). Additional clinical trials are required to evaluate a more precise correlation between flavonoid consumption and human health benefits (Burgess and Andrade, 2006). *Hypericum perforatum L.* attitude among the most significant phenolic rich dietary sources (Choi *et al.*, 2004; Lotito and Frei, 2006; Nogata *et al.*, 2006) with the induction of vascular cell adhesion molecules is a common feature in inflammatory environments. The suppressive effect of flavonoids on the expression of cell adhesion molecules in humans evaluated their antioxidative activity (Caristi *et al.*, 2003; Minato *et al.*, 2003).

Lemon (Citrus) juice contains such bifunctional components as flavonoids, carotenoids, and ascorbic acid (Gil-Izquierdo *et al.*, 2004). Eriocitrin (eriodictyol 7-O-rutinoside) and hesperidin (hesperetin 7-O-rutinoside) among the flavanone glycosides are found abundantly in lemon juice (Miyake, 2006). Eriocitrin has been reported to be a potent antioxidant and to have a suppressive effect on oxidative stress in streptozotocin-induced rats and acute exercise-induced rats (Shimoi *et al.*, 2000; Takaya *et al.*, 2003). Hesperidin has been reported to have anti-inflammatory and anti-hypertensive effects on experimental animals (Materska and Perucka, 2005; Pauli and Junior, 1995).

Although flavone glycosides and flavanone glycosides in *H. perforatum* have been analyzed by HPLC–DAD–MS/MS and by HPLC-ESI/MS (Gattuso *et al.*, 2006; Pauli and Junior, 1995). Some phenolic compounds in *H. perforatum* have not yet been identified and have not been examined for their functional activities. This study was undertaken to isolate and synthesize the polyphenolic compounds in lemon juice having radical scavenging activity. Hypericum has been reported to contain an abundance of flavanone glycosides as eriocitrin (216 mg/g of juice) and hesperidin (197 mg/g of juice) (Gil-Izquierdo *et al.*, 2002). Eriocitrin has been shown to have potent antioxidative activity for the inhibition of lipid auto-oxidation and a suppressive effect on oxidative stress in experimental animals (Erlund, 2004; Miyake *et al.*, 1997). Hesperidin 1 is reported to have hypertensive and anti-inflammatory effects, although it exhibits low antioxidative activity in comparison with eriocitrin (Caristi *et al.*, 2006; Gattuso *et al.*, 2007).

Further investigation of their biological importance demands sufficient quantities of well-defined compounds. To reach this target, we report in this article a convenient and concise synthetic approach for the preparation of chalcones 2 to 8. The synthesis of chalcone glycoside was reported (Oyama and Kondo, 2004) in which β-D- rhamnopyranosyl bromide was coupled with chalcone derivative which acts as aglycon acceptor under conventional glycosylation conditions. The objective of this study was to apply the smart method to obtain new important medicinal compounds from *H. perforatum*.

MATERIAL AND METHODS

The solvents used in these reactions were purified by distillation. Acetovanillone was purchased from Aldrich-Sigma Company. All reactions were run under argon atmosphere and monitored by TLC on 0.25-mm silica gel F254 plates (E. Merck) using UV light, and a 7% ethanolic solution of phosphor-molybdic acid and 5 % methanolic solution of sulphuric acid with heat as the coloration agent. Flash column chromatography was performed on silica gel (40-50 µm, Kanto reagents Co. Ltd. Silica-gel 60) to separate and purify the reaction products. Melting points were determined using an ASONE micro-melting point apparatus and uncorrected values were reported. IR spectra were recorded on a Horibal FT-720 IR spectrometer using a KBr disk. ^{1}H and ^{13}C NMR spectra were recorded on a JOEL ECX-500 spectrometer at 300 and 125 MHz respectively with chemical shifts being reported δ ppm from tetramethylsilane (TMS) as an internal standard. $CDCl_3$ (δ 7.21), D_2O (δ 4.80) CD_3OD (δ 3.31) and DMSO-d_6 (δ 2.49) were used as solvents.

The mass spectra were obtained by fast-atom bombardment (FAB) using 3-nitobenzyl alcohol (NBA) as a matrix and the JEOL JMS-AX505HA instrument. High-resolution mass spectra (HRMS) were obtained under electron spray ionization (ESI) conditions on a JEOL JMS-T100LP. Elemental analyses were performed on a Perkin-Elmer 2400 CHN elemental analyzer at the Microanalytical Center of Cairo University and all compounds were within ± 0.4 of the theoretical values (Rizk *et al.*, 2017).

Plant material

Seeds of *H. perforatum* L. were obtained from Sekem Company for biological products, El Salam City, Cairo, Egypt. The experiments were conducted in the plant tissue culture laboratory, Agricultural Botany Department, Faculty of Agriculture, Ain shams University, Shoubra El-Khaima, Cairo, Egypt, during the years of 2019-2020.

Callus initiation

For induction of callus from *H. perforatum* leaves, culture media containing 3% sucrose supplemented with various combinations of Kin, 2,4-D, BA, and NAA were used. A total of 4 different growth regulators combinations were prepared as follows: -

T1 (0.2 mg/l 2,4-D + 0.024 mg/l Kin)

T2 (0.22 mg/l 2,4-D + 0.024 mg/l Kin)

T3 (0.25 mg/l 2,4-D + 0.024 mg/l Kin)

T4 (0.22 mg/l 2,4-D + 0.5 mg/l BA + 0.1 mg/l NAA)

The pH value of the culture media was adjusted to 5.7 before autoclaving and add 0.7% agar. Culture media were dispensed into 150 ml jars which contained 25 ml of culture media. Autoclave sterilization (20 minutes, 121°C, and pressure equal to 1.5 atmospheres) was then carried out. Each treatment was represented by 10 replicates (jars) and each jar has 5 leaves as an explant. The culture was incubated at 25±2°C in full dark. Morphogenic responses were recorded after 4, 5, 6 weeks and the optimum hormonal combination for callus induction was determined.

Cell suspension culture

To produce cell suspension culture from callus, a fragment of the achieved callus was added to each 250 ml jar which contained 50 ml liquid media supplemented with the same hormonal

concentration that gave the best biomass of callus culture. The culture was incubated in growth rooms under controlled conditions, where the temperature was maintained at 25±2°C and subjected to shaking under 100 rpm, and incubated in the full dark for 4 weeks. For subculture, 2 ml from the previous cell suspension culture were sucked and injected into new jars containing the same liquid media.

Three different stimulants were added to different replicates of the new jars to increase the medicinal compound in the targeted cell suspension culture that will be produced. The stimulants used are yeast extract (0.25, 0.50 & 0.75 mg/L), emodin (5, 10 and 20 mg/L) and tyrosine (50, 100 & 150 mg/L). After 25 days samples of cell suspension were collected and the fresh weights were determined, then samples were dehydrated by the freezing device, then the dry weight was measured. The samples were then subjected to methanolic extraction. Accordingly, the most effective stimulant in extractions was determined by measuring the medicinal compounds by using an HPLC instrument.

Extraction of samples

Cell suspension cultures of *H. perforatum* were harvested washed and excessive water was removed. The harvest was then dried in shade. After constant weights were attained, one gram of dry fine cell suspension powders of different treatments was soaked in pure methanol (150 mL) separately at room temperature for 72 h with stirring from time to time. After that, filtration was carried out and the residue was washed with three successive rinses (100 mL) of pure methanol. The filtrate and washings were combined and evaporated to 10 mL.

The Hypericum was put into a reversed-phase column (È37 Â 500 mm, Amberlite XAD-2 resin, Rohm and Haas Co., Philadelphia, USA). The column was washed with 2-liter of water and eluted with 2-liter of 20% methanol; the eluate was then concentrated under reduced pressure. The concentrated extract was applied to HPLC (LC-8A, Shimadzu Co., Kyoto, Japan) which was carried out in a YMC-ODS column (YMC-Pack ODS-A, È20 Â 250 mm, S-5 mm, YMC Co., Kyoto, Japan) with UV detection of 330 nm, a mobile solvent of 20% methanol, and a flow rate of 10 ml/min at room temperature (Meignanalakshmi *et al.*, 2013).

2,6-Dihydroxy-4-*O*-(2,3,4,2',3',4'-hexa-*O*-benzyl-β-D-rhamnopyransoyl)-acetophenone (1).

To a solution of 2',4',6'-trihydroxy acetophenone (166.0 mg, 1.0 mmol) and per-*O*-benzyl-α-D-rhamnosyl bromide (1.23 g, 3.0 mmol) in quinoline (3.0 mL), Ag_2CO_3 (413.6 mg, 1.50 mmol) was added at 0°C and the mixture was stirred at 25°C in shaded conditions., TLC (hexane/ethyl acetate, 7/3, v/v) indicated completion of the reaction after stirring for 6 hours. MeOH was used to quench the reaction and the mixture was eluted through a short silica gel column with EtOAc. The eluent was evaporated to dryness. I N HCL (1ml) was added to the residue, and the mixture was extracted three times with AcOEt. The organic layer was washed with water, brine, and dried over anhydrous $MgSO_4$.

After evaporation under reduced pressure, the residual solid was purified by silica-gel column chromatography (n-hexane/AcOEt, 9.5/0.5 to 8/2, v/v) to afford 1 (481.6 mg, Y: 70%) as a yellow amorphous powder. IR (KBr): 3030, 2920, 2856, 1627, 1558, 1507, 1454, 1424, 1232, 1050, 735, 699 cm^{-1}; FAB-MS (*m/z*) 689.45 $(M+H)^{\cdot+}$ ^{1}H NMR (DMSO-d_6) δ: 11.13 (2H, bs, 2OH, acidic proton exchangeable D_2O), 7.71 (1H, dd, *J* =8.3, 2.0Hz, H-6), 7.61 (1H, d, *J* =2.0Hz, H-2), 7.53 (1H, d, *J* =8.3Hz, H-5), 7.42-6.90 (32H, m, Ar-H), 5.83 (1H, d, *J*=7.6Hz, H-1'), 4.69-4.43 (12H, m, 6CH_2Ph), 3.83 (1H, t, *J* =7.6Hz, H-2'), 3.82 (1H, t, *J* =8.9Hz, H-4'), 3.77-3.64 (1H, m, H-5'), 3.62 (1H, m, H-3'), 3.58-3.34 (2H, m, H-6'a,b), 2.57 (3H, s, CH_3CO); Anal. Calcd for $C_{62}H_{64}O_{13}$: C, 73.21; H, 6.34. Found: C, 72.91; H, 6.03.

5-Hydroxy-2-(3-hydroxy-4-methoxyphenyl)-7-((3,4,5-tris(benzyloxy)-6-(((3,4,5-tris(benzyloxy)-6-methyltetrahydro-2H-pyran-2-yl) oxy) methyl) tetrahydro-2H- pyran-2- yl) oxy) chroman-4-one (2).

To a solution of 1 (1.17 g, 1.70 mmol) and 3-hydroxy-4-methoxybenzaldehyde (0.502 g, 2.38 mmol) in 1,4-dioxane (10 mL), a 28% NaOMe-MeOH solution (10.0 mL) was added and the mixture was stirred at 25°C for 15 hours. The reaction mixture was poured into ice-cold 2N HCl solution (20 mL) and extracted with AcOEt three times. The combined extracts were washed with water, brine, dried over $MgSO_4$, and then subject to evaporation in vacuo. The residue was purified by flash-column chromatography on silica gel (7:1 hexane-AcOEt) to give 2 (36.34 mg, Y: 85%) as a viscous yellow oil, m.p 112-114, IR (KBr): 3030, 2868, 1624, 1579 cm^{-1}; ^1H NMR ($CDCl_3$) δ: 7.68 (1H, dd, *J* =8.2, 2.1Hz, H-6'), 7.64 (1H, d, *J* =15.4 Hz, *trans-vinyl* H), 7.62 (1H, d, *J* =2.1Hz, H-2'), 7.61 (1H, d, *J* =15.4Hz, *trans-vinyl* H), 7.58 (2H, d, *J* =8.9Hz, H-2, H-6), 7.51-6.71 (25H, m, Ar-H), 7.19 (1H, d, *J* =8.2Hz, H-5'), 6.78 (2H, d, *J* =8.9Hz, H-3, H-5), 5.51 (2H, s, ArOCH_2Ph), 4.90 (1H, d, *J* =9.7 H-1“), 4.85- 4.76 (4H, m, CH_2Ph), 4.51 and 4.18 (each 1H, d, *J* =12.1Hz, CH_2Ph), 4.35 (1H, br. t, *J* =9.7 Hz, H-2“), 4.04 and 4.10 (2H, d, *J* =12.1Hz, CH_2Ph), 3.89 (1H, s, 3'-OH), 3.45-3.66 (5H, m, H-3“,-4“,-5“,-6“a,b); FABMS (*m/z*) 883.32 $(M+H)^{.+}$ Anal. Calcd. for $C_{70}H_{70}O_{15}$: C, 73.03; H, 6.13. Found: C, 72.76; H, 5.91.

5-Hydroxy-2-(3-hydroxy-4-methoxyphenyl)-7-((3,4,5-trihydroxy-6-(((3,4,5-trihydroxy-6-methyltetrahydro-2H-pyran-2-yl)oxy)methyl)tetrahydro-2H-pyran-2-yl)oxy)chroman-4-one (3)

To a solution of 2 (0.120 g, 0.15 mmol) in MeOH (3.0 mL) and AcOEt (3 mL) was added 10 wt % of Pd $(OH)_2$ / C (30 mg). The suspension was vigorously stirred under H_2 atmosphere for 5 hours at 25. The catalyst was then removed by filtration using Celite, followed by washing with MeOH. The filtrate was evaporated in vacuo and purified by flash column chromatography on silica gel (5:1 $CHCl_3$/MeOH) to afford 3 as a white amorphous powder (31.29 mg, 64%), m.p. 134-136, IR (film): 3368, 3010, 2920, 2850, 1650, 1594cm^{-1}; ^1H NMR (CD_3OD) δ: 7.74 (β, d, *J* =15.2Hz), 7.71 (1H, dd, *J* =8.1, 2.1Hz, H-6'), 7.65 (2H, d, *J* =8.8Hz, H-2, H-6), 7.61 (1H, d, *J* =2.1Hz, H-2'), 7.57 (α, d, *J* =15.2Hz), 7.21 (1H, d, *J* =8.1Hz, H-5'), 6.95 (2H, d, *J* =8.8Hz, H-3, H-5), 5.04 (1H, d, *J*=7.6Hz, H-1“), 3.89 (3H, s, 3'-OCH_3), 3.80 (3H, s, 4-OCH_3), 3.53 (1H, t, *J* =7.6Hz, H-2“), 3.49-3.45 (2H, m, H-3“, H-5“), 3.40 (1H, t, *J* =8.9Hz, H-4“), 3.88 (1H, dd, *J* =12.4, 2.1Hz, H-6“a), 3.68 (1H, dd, *J* =12.4, 6.2Hz, H-6“b); FABMS: *m/z* 447.16 $[M+H]^{.+}$, Anal. Cal. for $C_{28}H_{34}O_{15}$: C, 55.08; H, 5.61. Found: C, 54.81; H, 5.39.

4-(5-Hydroxy-4-oxo-7-((3,4,5-tris(benzyloxy)-6-(((-3,4,5-tris(benzyloxy)-6-methyltetrahydro-2H-pyran-2-yl) oxy) methyl) tetrahydro-2H-pyran-2-yl) oxy)chroman-2-yl) -5-phenyl-2,4-dihydro-3H-pyrazol-3-one (4).

To a solution of 1 (1.17 g, 1.70 mmol) and 5-phenylpyrazol-3-on-4-carboxaldehyde (0.502 g, 2.38 mmol) in 1,4-dioxane (10 mL), a 28% NaOMe-MeOH solution (10.0 mL) was added and the mixture was stirred at room temperature for 15 h. The reaction mixture was poured into ice-cold 2N HCl solution (20 mL) and extracted three times with AcOEt. The combined extracts were washed with water, brine, dried over $MgSO_4$, and then subjected to evaporation in vacuo. The residue was purified by flash-column chromatography on silica gel (7:1 hexane-AcOEt) to give 4 (1.42 g, Y: 95%) as a viscous yellow oil, m.p. 154-156, IR (KBr): 3030, 2868, 1624, 1579 cm^{-1}; ^1H NMR ($CDCl_3$) δ: 12.43 (1H, s, NH, acidic proton exchangeable D_2O), 10.13 (1H, s, OH, acidic proton exchangeable D_2O), 7.51-6.71 (35H, m, Ar-H), 7.19 (1H, d, *J* =5.2Hz, H-5' chromone), 6.78 (1H, d, *J* =5.2Hz, H-7'chromone), 5.51 (4H, s, $ArOCH_2Ph$), 4.90 (2H, d, *J* =9.7, H-1', H-1“), 4.85- 4.76 (8H, m, OCH_2Ph), 4.68 (4H, s, *J* =8.2, 2.1Hz, H-6', H-6"), 4.62-4.61 (1H, d, *J* =2.1Hz, H-2', H-2"), 4.58-4.55 (2H, d, *J* =8.9Hz, H-3', H-3"), 4.35 (2H, br. t, *J* =9.7 Hz, H-2', H-2“),3.45-3.66 (4H, m, H-5',-4“,-5“,-4'); FABMS (*m/z*) 1187.32 $(M+H)^{.+}$ Anal. Calcd. for $C_{72}H_{70}N_2O_{15}$: C, 72.83; H, 5.94; N, 2.36. Found: C, 72.56; H, 5.71; N, 2.04.

4-(5-Hydroxy-4-oxo-7-((3,4,5-trihydroxy-6-(((3,4,5-trihydroxy-6-methyltetrahydro-2H-pyran-2-yl)oxy)methyl)tetrahydro-2H-pyran-2-yl)oxy)chroman-2-yl)-5-phenyl-2,4-dihydro-3H-pyrazol-3-one (5)

To a solution of 4 (0.120 g, 0.15 mmol) in MeOH (3.0 mL) and AcOEt (3 mL) was added 10 wt % of Pd $(OH)_2$ / C (30 mg). The suspension was vigorously stirred under H_2 atmosphere for 5 h at room temperature. The catalyst was then removed by filtration through Celite, followed by washing with MeOH. The filtrate was evaporated in vacuo and purified by flash column chromatography on silica gel (5:1 $CHCl_3$/MeOH) to afford **5** as a white amorphous powder (36.23 mg, 73%). IR (film): 3368, 3010, 2920, 2850, 1650, 1594cm-1; FABMS: *m/z* 447.16 $[M+H]^{+}$ ^1H NMR (CD_3OD) δ: 12.27 (1H, s, NH, acidic proton exchangeable D_2O), 10.62 (1H, s, OH, acidic proton exchangeable D_2O), 7.74-6.72 (7H, m, ArH), 6.53-6.52 (β, d, *J* =15.2Hz), 5.71-5.69 (1H, dd, *J* =8.1, 2.1Hz, H-6'), 5.65-5.64 (2H, d, *J* =8.8Hz, H-2, H-6), 5.61-5.60 (1H, d, *J* =2.1Hz, H-2'), 5.57-5.56 (α, d, *J* =15.2Hz), 5.21-5.20 (1H, d, *J* =8.1Hz, H-5'), 4.95 (2H, d, *J* =8.8Hz, H-3, H-5), 4.42-4.41 (1H, dd, *J* =7.9Hz, enanteotopic CH pyraz), 4.34-4.32 (1H, d, *J*=7.6Hz, H-1“),4.12-4.11 (1H, dd, *J* =7.9Hz, enanteotopic CH chromone), 3.92-3.90 (2H, dd, *J* =7.9Hz, diastereotopic CH_2 chromone), 3.80 (2H, s, OCH_2), 3.53 (1H, t, *J* =7.6Hz, H-2“), 3.49-3.45 (2H, m, H-3“, H-5“), 3.40 (1H, t, *J* =8.9Hz, H-4“), 3.88 (1H, dd, *J* =12.4, 2.1Hz, H-6“a), 3.68 (1H, dd, *J* =12.4, 6.2Hz, H-6“b); FABMS (*m/z*) 647.43 $(M+H)^{+}$ Anal. Calcd for $C_{30}H_{34}O_{14}$: C, 55.73; H, 5.30; N, 4.33. Found: C, 55.41; H, 5.09; N, 4.00.

Computational methods

DFT studies were carried out for the compounds (1-8) using Materials Studio 6.0 (MS 6.0) software from Accelrys, Inc. $DMol^3$ module was used to perform the DFT calculations using Perdew and Wang LDA exchange-correlation functional and DND basis set. The calculated parameters involved the electron density, dipole moment, frontier molecular orbitals, and molecular surface area. Frontier molecular orbitals include the highest occupied molecular orbitals (HOMOs) and the lowest unoccupied molecular orbitals (LUMOs) (Lotito and Frei, 2006).

RESULTS AND DISCUSSION

Effect of different growth regulators and incubation period on the fresh weight of *H. perforatum* callus

It could be observed that both the fresh and dry weight of the callus took the same trend. The results indicated that the general tendency of all growth parameters as overall mean was to gradually increase significantly and decrease by increasing incubation period. The highest positive growth regulator effect on callus fresh weight and dry weight (0.2430 and 0.0175g) respectively was found at T2 while the best incubation period effect on callus fresh and dry weights (0.2118 and 0.0167g) respectively was found at 5 Weeks. Results are illustrated in Tables (1 and 2) as below. The maximum values of callus fresh and dry weight were recorded after an incubation period of 5 weeks on T2 treatment (0.3066 and 0.0235 g), respectively. In this respect, the highest cell growth was obtained from explants cultivated in the presence of 4.4 µM BA and 4.5 µM 2,4-D in the dark (Pretto and Santarém, 2000).

Also, it reported the highest frequency of callus induction from the leaf discs explant cultivated on the medium with 30 g l^{-1} of sucrose, 0.5 mg l^{-1} of 2,4- D, and 0.5 mg l^{-1} of kinetin. According to previous studies, 2,4-D and kinetin consider effective plant growth regulators for callus induction and cell suspension cultures from *H. perforatum* L. (Ayan *et al.*, 2005; Walker *et al.*, 2002). Results documented in Table (3) represent the effect of yeast extract, emodin, and tyrosine on the cell suspension culture of *H. perforatum* fresh and dry weight (g) after a 25-day incubation period. The results indicated that the general tendency of all growth parameters as overall mean was to gradually increase significantly by increasing the concentration of yeast extract and emodin, while decrease by increasing the concentration of tyrosine.

Table 1. Effect of different growth regulators and incubation period on fresh weight of callus of *H. perforatum*.

The incubation period (week)	Fresh weight (g)				Mean
	T1	T2	T3	T4	
4	0.0987^{j}	0.1522^{f}	0.1405^{g}	0.0827^{k}	0.1185^{C}
5	0.1904^{c}	0.3066^{a}	0.1736^{e}	0.1736^{e}	0.2118^{A}
6	0.1369^{h}	0.2702^{b}	0.1255^{i}	0.0608^{l}	0.1483^{B}
Mean	0.1420^{C}	0.2430^{A}	0.1475^{B}	0.1057^{D}	

Means followed by different letters are significantly different at LSD 5%. Capital letters for the mean of overall treatment or incubation period, whereas lowercase letters for interaction.

Table 2. Effect of different growth regulators and incubation period on the dry weight of callus of *H. perforatum*.

The incubation period (week)	Fresh weight (g)				Mean
	T1	T2	T3	T4	
4	0.0116^{g}	0.0142^{d}	0.0130^{f}	0.0048^{l}	0.0109^{B}
5	0.0118^{g}	0.0235^{a}	0.0167^{b}	0.0146^{cd}	0.0167^{A}
6	0.0064^{h}	0.0149^{c}	0.0137^{e}	0.0049^{j}	0.0100^{C}
Mean	0.0099^{C}	0.0175^{A}	0.0145^{B}	0.0081^{D}	

Means followed by different letters are significantly different at LSD 5%. Capital letters for the mean of overall treatment or incubation period, whereas lowercase letters for interaction.

Table 3. Effect of yeast extract, emodin, and tyrosine on the cell suspension culture of Hypericum perforatum fresh and dry weight (g) after a 25-day incubation period.

Treatments	Concentration			Mean
Yeast extract	0.25 mg/l	0.50 mg/l	0.75 mg/l	
F.W.	0.68^{c}	0.80^{b}	1.00^{a}	0.116
D.W.	0.04	0.05	0.05	N.S.
Emodin	5 mg/l	10 mg/l	20 mg/l	
F.W.	0.83^{b}	0.84^{b}	0.87^{a}	0.024
D.W.	0.05^{b}	0.06^{b}	0.14^{a}	0.020
Tyrosine	50 mg/l	100 mg/l	150 mg/l	
F.W.	0.83^{a}	0.73^{b}	0.70^{c}	0.028
D.W.	0.04	0.04	0.04	N.S.

Means followed by different letters are significantly different at LSD 5%.

On the positive side, the maximum significant values of callus fresh weight recorded with yeast extract were 1.00 g at mg l^{-1}, with emodin was 0.87 g at 20 mg l^{-1} and with tyrosine was 0.83 g at 50 mg l^{-1}. There is no significant difference between the callus dry weight in both yeast extract and tyrosine while found positive significance in emodin treatment and the highest one was 0.14 g with 20 mg l^{-1}.

These results are consistent with the results on the role of yeast extract in redoubling the callus growth, this is due to being rich in effective constituents, like amino acids, peptides, low-molecular-weight organic matter, nucleotides, nitrogen, phosphorus, and trace elements (Jaddoa and Ibrahim, 2014; Xi *et al.*, 2019). A similar result was also reported in *Silybum marianum* where tyrosine 10 mg l^{-1} significantly increased callus fresh weight. The L-tyrosine is the hydroxyl phenol acid, one of the amino acids utilized as advancing development which is utilized to build proteins, hormones, and an

important source for different plant components. It has a vital role as a precursor of thousands of vital and specialized compounds in plant cells (Bakry *et al.*, 2020; Rabie *et al.*, 2010).

Chemistry

The fraction eluted with methanol by reversed-column chromatography of *H. perforatum* L. cell suspension was examined for its antioxidative activity by using a linoleic acid oxidation system (Hara *et al.*, 2011). The fraction eluted with 20% methanol exhibited antioxidative activity, although this was lower than the activity with 40% methanol which contained eriocitrin and hesperidin 1 (De Jong and Borm, 2008). However, phenolic compounds of hydrophilic antioxidants seemed to be present in the fraction with 20% methanol. We attempted in this study to isolate the phenolic compounds in the fraction eluted with 20% methanol and to identify them because hydrophilic functional compounds can be expected to apply to drinks and water-soluble foods. *H. perforatum* L. cell suspension was outlined via HPLC-MS spectrometry (Figures 1 and 2) supported by different synthetic approaches as a candidate for constructing the target chalcone glycosides 2, 3 as delineated in (Scheme 1).

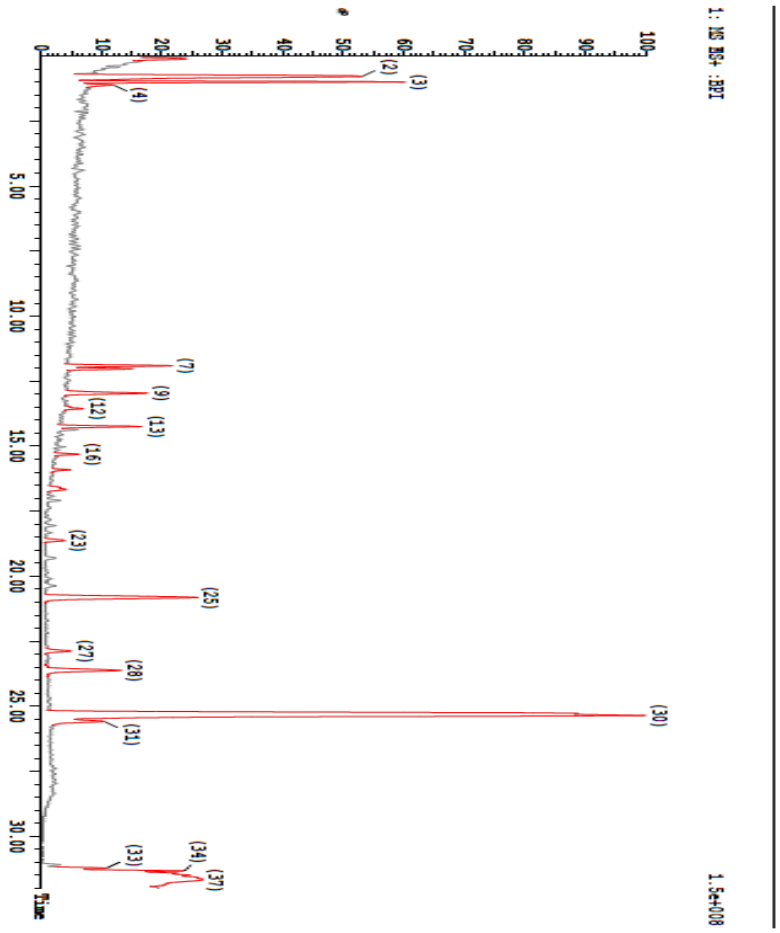

Fig. 1. Outline HPLC pattern for *H. perforatum* L. extracted by 20% methanol.

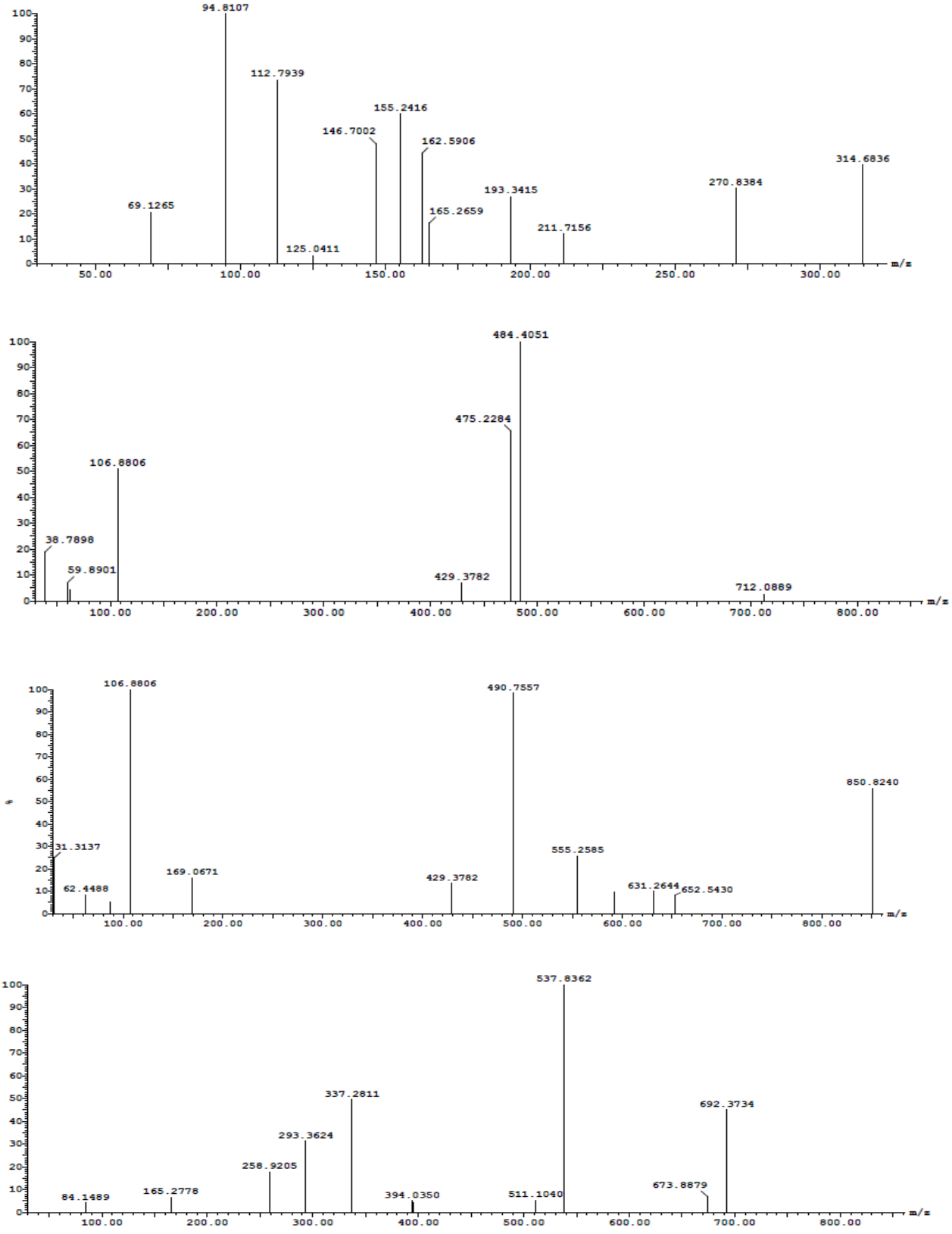

Fig. 2. Outline the mass pattern for the major chemical constituents for *H. perforatum* L.

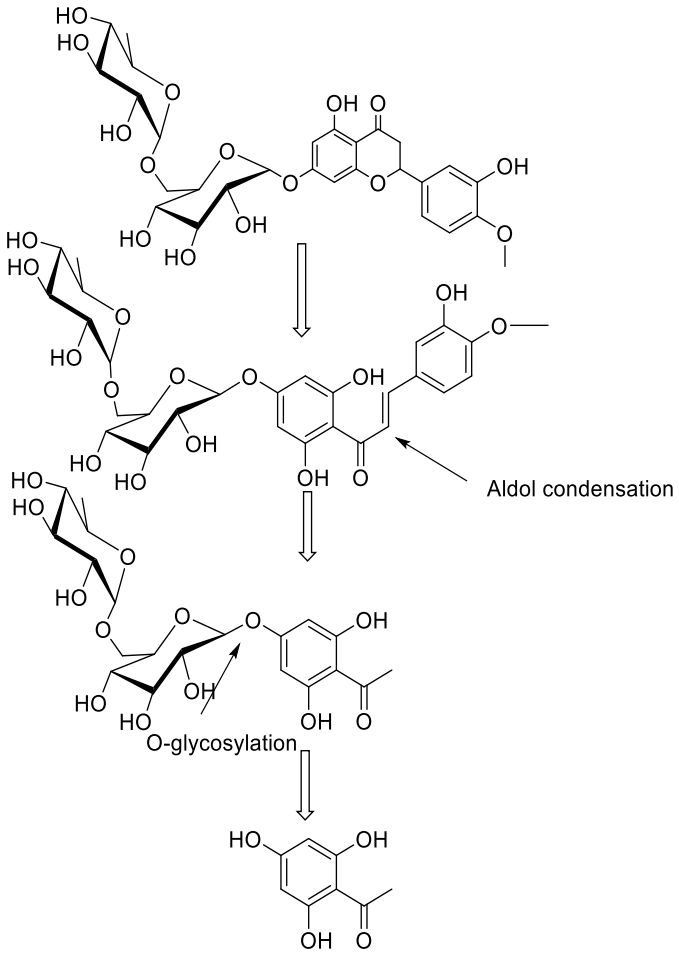

Scheme 1. Retrosynthetic plan of hesperidin (hesperetin 7-Orutinoside) synthesis (Rizk *et al.*, 2018a).

This approach includes three steps:

i) *O*-glucosylation of 4-OH of 4'-hydroxy-3'-methoxy acetophenone (commercially known as Acetovanillone); when 1.0 equivalent of per-*O*-benzyl-α-D-rhamnosyl bromide (El-Hashash *et al.*, 2015) as a donor (E_{HOMO} = -1.20) was reacted with 2.0 equivalents of 2',4',6'-trihydroxy-acetophenone as acceptor (E_{LUMO} =-3.20) in quinoline in the presence of 1.5 equivalents of Ag_2CO_3 and powdered molecular sieves 4Å. Formation of acetophenone glycoside derivative 1 with high β selectivity (α/β = 1/5, 70%) was achieved due to the presence of the insoluble silver salt which restricted the anomerisation of the bromide ion allowing the reaction to proceed with an inversion in configuration (El-Hashash and Rizk, 2017; Elkholy *et al.*, 2019; Heakal *et al.*, 2017; Rizk *et al.*, 2018b) (Scheme 2 outline the proposal mechanism via DFT view).

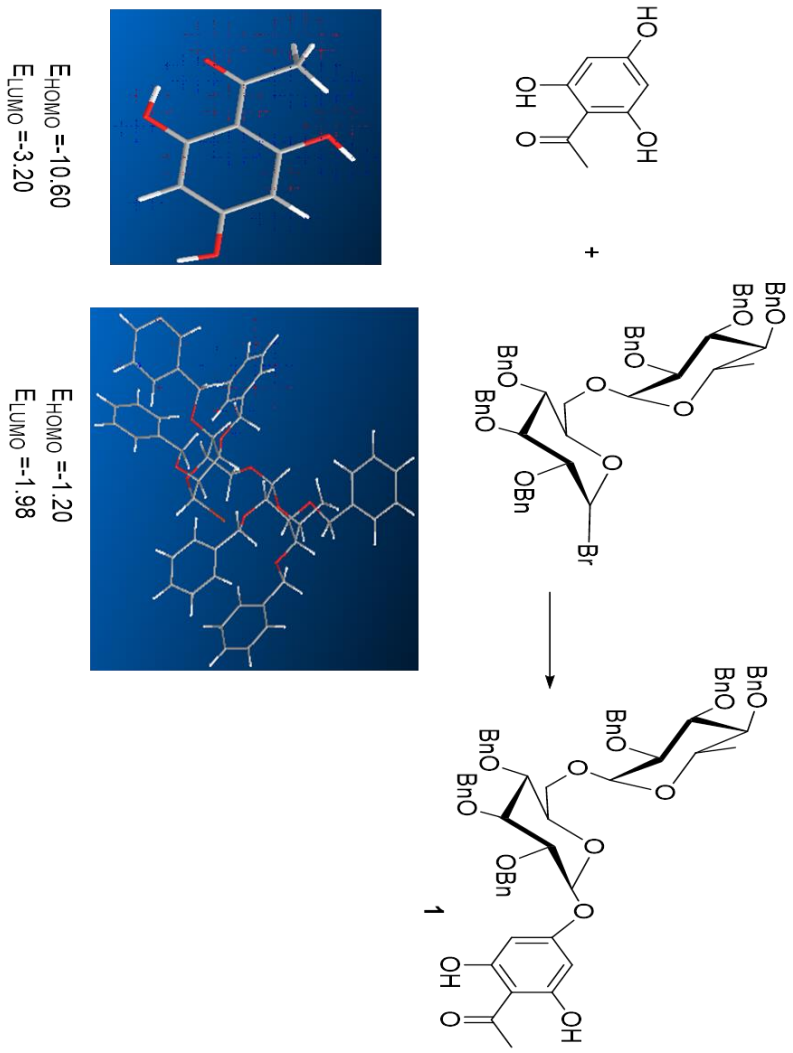

Scheme 2. The proposal mechanism via DFT view (El-Hashash and Rizk, 2017; Elkholy *et al.*,, 2019; Heakal *et al.*,, 2017; Rizk *et al.*,, 2018b).

ii) Introduction of the vanillin (4-hydroxy-3-methoxy benzaldehyde) and 5-phenylpyrazo-3-one-4-carboxaldehyde residue by aldol condensation; in which the LUMO energy of vanillin (E = -4.81 eV) is more reactive than the pyrazole aldehyde (E=-2.59 eV) when they reacted with the glycoside 1 (HOMO -7.60 eV) (Scheme 3).

iii) Full debenzylation of the isomers 2 and 3 of all the sugar hydroxyl groups occur to afford chalcone followed by cyclization yielding the chromone glycosides 4 and 5 respectively (Schemes 4 and 5).

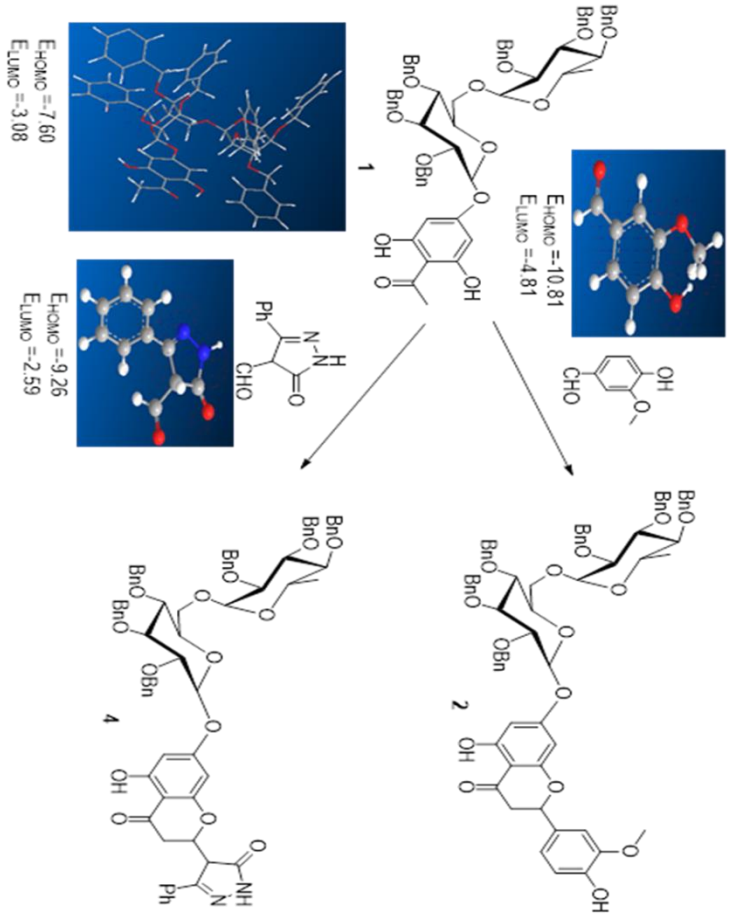

Scheme 3. Outline LUMO energies of the aldehydes are being attacked by HOMO energy of the glycoside 1 (Rizk *et al.,*, 2018b).

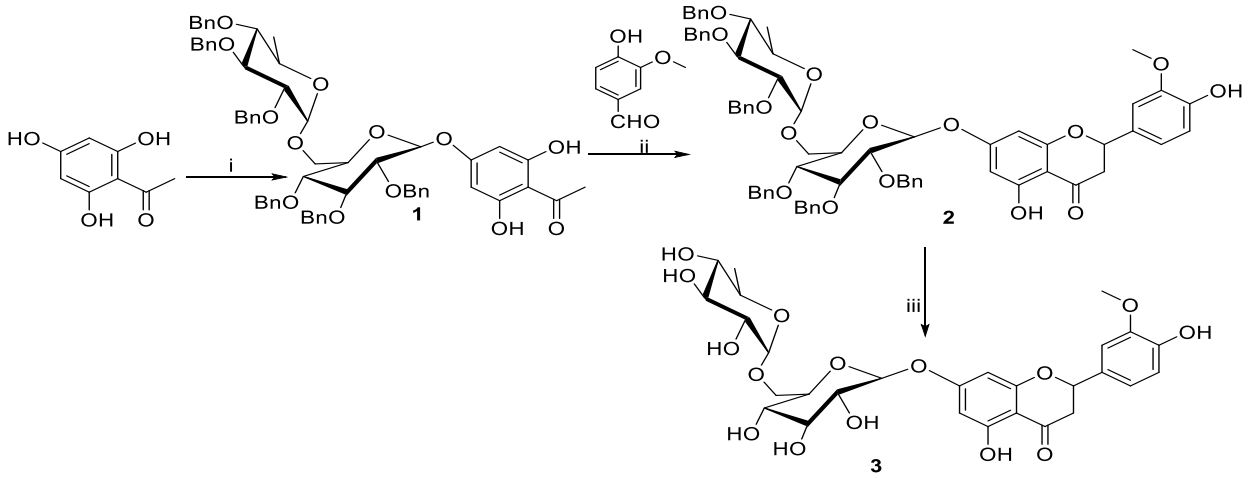

Scheme 4. Reagents and conditions i) per-O-benzylrhamnosyl bromide (3 equiv.), Ag_2CO_3 (1.5 equiv.) in quinoline 0^oC -rt, 6h. ii) NaOMe (1.5 equiv.) in dioxane, rt, 2 hr iii) H2/10% Pd (OH)2, AcOEt / EtOH (1:1), 4h (Rizk *et al.,*, 2018b).

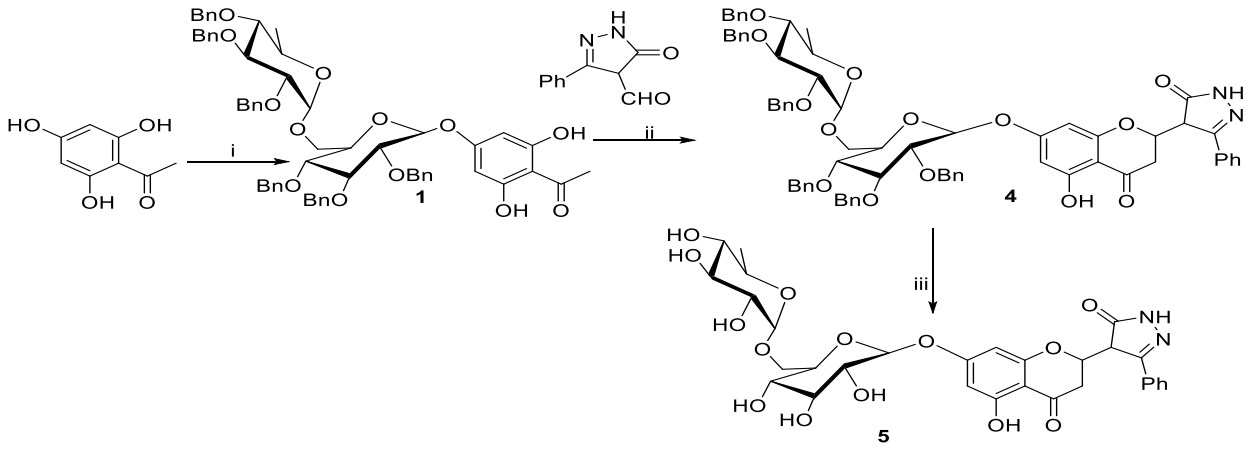

Scheme 5. Reagents and conditions i) per-O-benzylrhamnosyl bromide (3 equiv.), Ag_2CO_3 (1.5 equiv.) in quinoline 0^oC -rt, 6h ii) NaOMe (1.5 equiv.) in dioxane, rt,2 h iii) H_2/10% Pd $(OH)_2$, AcOEt / EtOH (1:1), 4h (Rizk *et al.,*, 2018b).

Stereoselective *O*-glycosylation to have mainly β-glycosylation was carried out via Koenigs-Knorr reaction using the procedure established by Oyama (De Jong and Borm, 2008; Hara *et al.,*, 2011). The appearance of bands at 3434, 3329 attributed to NH_2 asymmetric and symmetric stretching frequency in the IR spectrum of **5** are good evidence for the structure assigned to this compound; the 2221 cm^{-1} band is due to the presence of the CN group, in addition to the C=O group at 1732 cm^{-1} corresponding to the carbonyl of the coumarin ring. Its ^{1}H-NMR spectrum displays specific signals for pyridine protons at position 3 that appeared at δ 6.80 ppm, while the singlet due to the NH_2 protons are observed at δ 4.22 ppm and the absence of a specific CH_3 signal. The signal of the NH proton is observed at δ 9.80 ppm as a singlet.

DFT-based characterization

Quantum mechanical program was used for the molecular parameters and the fully optimized minimum energy geometrical configuration of the oxidative inhibitor. It is well known that high E_{HOMO} is likely to indicate a strong tendency of the molecule to donate electrons. The low values of the energy gap ($\Delta E=E_{LUMO}–E_{HOMO}$) will render good inhibition efficiencies because the energy needed to remove an electron from the last occupied orbital will be low (Hussein *et al.*, 2018; Rizk *et al.*, 2019; Rizk *et al.,*, 2018a; Rizk *et al.,*, 2017). The ΔE of a molecule is a measure of the hardness or softness of a molecule. Hard molecules are characterized by larger values of ΔE and vice versa. The linear correlation between E_{HOMO} energy level and the oxidation inhibition efficiency of the inhibitors proved that the higher the HOMO energy (less negative values) of the inhibitor or antioxidant, the greater the trend of offering electrons. The order of increasing E_{HOMO}, decreasing E_{LUMO} values, and the energy gap (ΔE) are directly proportional to increasing efficiency. The tendency of an electron cloud to be distorted from its normal shape is referred to as its polarizability, the greater the polarizability the more inhibitor molecules will leave from solvent

bulk to be absorbed by a radical or oxidized surface to form a protective film, we can consider the polarizability as a resultant of all intramolecular electron transfer interactions. This increased volume enhances the ease of the distortion of the electron cloud which will promote the adsorption of the chromone. DFT-based quantum calculations can give insights into the structural and electronic characteristics of organic molecules (Attia *et al.*, 2019). Herein, the parameters obtained from the DFT study performed for chromone glucosides derivatives 1-3 are the energies of Frontier molecular orbitals. HOMOs are the regions at which the electrophilic attack occurs, whereas the LUMO represent the sites of nucleophilic attack (Azab *et al.*, 2016). The HOMO energy (E_{HOMO}) is a parameter of direct relation to the ionization potential and its value expresses the susceptibility of the organic molecule towards attacks by electrophiles. Unlikely, the LUMO energy (E_{LUMO}) refers to the electron affinity and its value expresses the vulnerability of the molecule towards a nucleophilic attack. To obtain these parameters, the molecule must be subjected first to geometry optimization, and then these parameters are calculated. The HOMO and LUMO distributions are displayed in Scheme 3. The obtained E_{HOMO} and E_{LUMO} of the synthesized compounds are listed in Table 1. The listed results indicate that the values of gap energy (ΔE), where $\Delta E = E_{LUMO} - E_{HOMO}$, follow the order: chromone glucoside 1 < chromone glucoside 2 < chromone glucoside 3. Compounds having small ΔE values are generally referred to as soft compounds, while those having large values are called hard compounds. In general, soft compounds are more reactive towards metal-additive interactions; being capable of donating electrons easily to the metal surface (El-Hashash *et al.*, 2011). Generally, for organic material to interact effectively with the metal surface, it must contain heteroatoms rich in non-bonded electrons (free lone pairs) and/or aromatic rings having p-electrons. The synthesized compounds under study are rich in O and N atoms containing free lone pairs of electrons beside double bonds and aromatic rings containing p-electrons. Low-gap-energy compounds generally provide good interaction as an antioxidant because the energy required to remove an electron from the last occupied orbital (HOMO) of the inhibitor will be minimized and it will be easy to donate electrons to metal and they can be easily polarizable more than hard compounds (Miyake, 2006). Several other various quantum chemical parameters can help to predict the molecular characteristics of chromone additives such as ionization potential (I), electron affinity (A), absolute electronegativity (***χ***) and absolute chemical hardness (*η*) be sure these arrange the binding according to Chromone glycoside 2 < Chromone glycoside 3 < Chromone glycoside 1. ***χ*** and *η* are two quantities related to I and A, where ***χ*** = I+A/2 and ***η*** = I-A/2, I and A are calculated in turn, from E_{HOMO} and E_{LUMO}, where $I = -E_{HOMO}$ and $A = -E_{LUMO}$. For any two molecules in contact with each other, electrons will be partially transferred from the one of low value to that of higher value. Chromone 2 where it has the highest value of chemical softness (s), which is defined as the inverse of hardness ($s = 1/ \boldsymbol{\eta}$) (Erlund, 2004). The electrophilicity ω index is given by the simple expression: $\omega = E^2/ \eta$. The electrophilicity ω index encompasses the tendency of an electrophile to acquire an extra amount of electron density, given by binding

energy (E) and the resistance of a molecule to exchange electron density with the environment, given by η. Thus, a good electrophile is a species characterized by a high (E) value and a low (η) value. Besides, the maximum number of electrons that an electrophile can acquire is given by the expression: $\Delta N_{max} = E/\eta$. Hence, chromone glycosides 1, 2, and 3 are predicted to be the best powerful additive as antidepressant agents.

The optimized geometries of compounds displayed wholly distributed over every molecular structure (Figure 1) in addition to Frontier molecular orbitals possess the highest occupied molecular orbital (HOMO) and the lowest unoccupied molecular orbital (LUMO) beside their surface area. The regions of the highest electron density (HOMO) represent the electrophilic-attacking sites, whereas the LUMO reflects the nucleophilic-attacked sites (Pauli and Junior, 1995). As the dipole moment (μ) is a promising measurable parameter for the molecular polarity, it is evident from Table 1 that compounds **2** exhibits high polarities and the nucleophilicity index (ω) as well as the hydration energy, follow the order: **2** > **5** > **3** > **4** conform the yield % of Mannich products. Accordingly, the DFT data run in harmony with the previously obtained results (cf. Table 4).

Structure-activity relationships (SARs)

The evaluation of the antidepressant activities of the newly synthesized compounds **2**-**5** demonstrated the presence of electron-withdrawing groups in the observed activities in vitro. The most potent thiouracil compounds **2, 3**, **4,** and **5** contain heterocyclic rings and electron-withdrawing moieties. Moreover, antifungal evaluation displayed conflicting results, considering that compounds having electron-withdrawing substituents had weak inhibitory activities.

Also, the data represented in Table 4 showed that compounds 2-5 possess a pronounced antibacterial activity against *Staphylococcus aureus, Bacillus subtilis,* and *Escherichia coli* compared to the reference drug penicillin. As far as antifungal activity is concerned, compounds **2** exhibited promising activity, which equals to reference drug *Colitrimazole* against *Candida albicans* and compounds 3, 4, and 5 against *Aspergillus flavus.* Compounds 4 and 5 showed moderate activity against the fungus *Candida albicans* and compounds 4 and 5 displayed moderate activity against the fungus *A. flavus*. Compounds 2, 3, 4, 5 were either inactive or moderately active against the tested bacteria. Chromone 4 and 5 have lower antimicrobial activity, although presenting chemical structures similar to compound 2 (highest antimicrobial activity). DFT studies indicate that compounds 2 and 3 have higher HOMO energies, which can be correlated to their lower antimicrobial activities (Erlund, 2004; Miyake *et al.,*, 1997).

Table 4 shows that the HOMO energies for such compounds follow the order: 2 > 5 > 4. Compounds 3, 4, and 5 showed the highest antibacterial activity whereas compound 3 exhibited excellent results against *C. albicans* and *A. flavus*. The structure-activity relationship suggested that thiouracils containing amide or hydrazide moiety showed higher antibacterial and antifungal activities than other derivatives (Caristi *et al.,*, 2006; Gattuso *et al.,*, 2007).

The present study revealed that conversion of thiol group at 5'-position to hydrazide **9** caused a pronounced inhibition effect against Gram-positive (*Staphylococcus aureus, Bacillus subtilis*) and Gram-negative (*Escherichia coli*) bacteria. Compounds **3**, **4,** and **5** exhibited the highest lipophilicity, charge density, and surface area among the newly synthesized thiouracil derivatives, as revealed by DFT. These hydrophobic compounds were most potent against *E. coli*, *S. aureus*, and *C. albicans*.

DFT-based QSAR e.g. high molecular weight (ADME), electron-withdrawing groups (low HOMO values) and shape indexes in structure-property modeling (high kappa index) (Oyama and Kondo, 2004) of such compounds supported the high antimicrobial activity (c.f. Table 4).

Table 4. Global reactivity indices and energy level distribution of frontier orbitals, ionization potential, electron affinity, chemical potential, hardness, electrophilicity index, nucleophilicity index, and softness.

Compound	E_{HOMO} (eV)	E_{LUMO} (eV)	ΔE (eV)	I (eV)	A (eV)	E_{Bind} (eV)	χ (eV)	η (eV)	S (eV^{-1})	ω	ε	ΔN
(1)	-10.22	-3.21	7.01	4.302	1.945	-3.123	3.123	2.357	0.424	2.07	0.48	1.32
(2)	-3.05	-2.70	0.35	4.133	1.945	-3.039	3.039	2.188	0.457	2.11	0.47	1.38
(3)	-10.62	-3.21	7.41	4.428	1.931	-3.179	3.179	2.497	0.400	2.02	0.49	1.27
(4)	-9.22	-3.19	6.03	8.33	0.63	-5.13	-4.25	2.25	5.24	1.23	0.43	1.12
(5)	-9.23	-3.18	6.05	4.98	0.43	-4.87	-4.23	4.24	6.38	2.00	0.39	1.32

CONCLUSION

Flavone-7-glycosides in the *Hypericum perforatum* L. was suggested to be the most effective chemical constituents as an antidepressant and antimicrobial agent because it contains abundantly bioactive compounds having a suppressive effect on the expression of blood adhesion molecules. This study found the bioactive compounds of phenolic glucosides in the fractionation and extracted hypericum herbs. DFT bases quantum chemical computational and electron impact mass spectra can be revealed the characterization of the chromone glycosides in the hypericum extract. Also, we have described a simple and practical synthetic procedure by which chalcones 1, 2, and 3 were synthesized in an overall yield of 13%, 14%, and 90% respectively. This concise proposed synthetic route of those simple chalcone glycosides could be utilized to be a viable procedure for the synthesis of various *O*-diglycosyl chalcones.

ACKNOWLEDGMENT

We thank the Botany department, Faculty of Agriculture and Chemistry Department, Faculty of Science, Ain-Shams University, Egypt which financially supported this work. Deep thanks and appreciation are devoted to the Scholar Rescue Fund – Institute of International Education (IIE-

SRF) for allowing the fellowship and providing the required fund for my researches.

CONFLICT OF INTEREST

There is no conflict of interest.

REFERENCES

Al- Mahweety, J.A.N., 2016. Phytochemical Studies on Medicinal Plants, Dracaenaceae resin, of Socotra Island, Yemen. PSM Biol. Res., 1(2): 62-65.

Ali, K., Shuaib, M., Ilyas, M., Hussain, F., Hussain, F., 2017. Medicinal Uses of Chemical Extracts from *Withania somnifera* and Its Antimicrobial Activity: A Mini-Review. PSM Microbiol., 2(1): 20-23.

Amin, R.A., Edris, S.N., 2017. Grape Seed Extract as Natural Antioxidant and Antibacterial in Minced Beef. PSM Biol. Res., 2(2): 89-96.

Asres, K., Seyoum, A., Veeresham, C., Bucar, F., Gibbons, S., 2005. Naturally derived anti-HIV agents. Phytother. Res., 19(7): 557-81.

Attia, S., Elgendy, A., Rizk, S., 2019. Efficient green synthesis of antioxidant azacoumarin dye bearing spiro-pyrrolidine for enhancing electro-optical properties of perovskite solar cells. J. Mol. Struct., 1184: 583-592.

Ayan, A.K., Çirak, C., KEVSEROĞLU, K., Sökmen, A., 2005. Effects of explant types and different concentrations of sucrose and phytoharmones on plant regeneration and hypericin content in *Hypericum perforatum* L. Turk. J. Agric. For., 29(3): 197-204.

Azab, M.E., Rizk, S.A., Mahmoud, N.F., 2016. Facile synthesis, characterization, and antimicrobial evaluation of novel heterocycles, schiff bases, and N-nucleosides bearing phthalazine moiety. Chem. Pharm. Bull., 64(5): 439-450.

Bakry, b.a., Sadak, M., El-Monem, A., 2020. Physiological Aspects of Tyrosine and Salicylic Acid on Morphological, Yield and Biochemical Constituents of Peanut Plants. Pak. J. Biol. Sci., 23: 375-384.

Benavente-García, O., Castillo, J., Marin, F.R., Ortuño, A., Del Río, J.A., 1997. Uses and Properties of Citrus Flavonoids. J. Agric. Food Chem., 45(12): 4505-4515.

Bito, T. et al., 2002. Flavonoids differentially regulate IFN gamma-induced ICAM-1 expression in human keratinocytes: molecular mechanisms of action. FEBS Lett., 520(1-3): 145-52.

Burgess, J.R., Andrade, J.E., 2006. Antioxidant effects of citrus flavonoid consumption, Potential health benefits of Citrus (ACS Symp. Ser. 936), pp. 161-174.

Caristi, C., Bellocco, E., Gargiulli, C., Toscano, G., Leuzzi, U., 2006. Flavone-di-C-glycosides in citrus juices from Southern Italy. Food Chem., 95(3): 431-437.

Caristi, C. et al., 2003. Flavonoids detection by HPLC-DAD-MS-MS in lemon juices from Sicilian cultivars. J. Agric. Food Chem., 51(12): 3528-34.

Choi, J.-S., Choi, Y.-J., Park, S.-H., Kang, J.-S., Kang, Y.-H., 2004. Flavones mitigate tumor necrosis factor-α-induced adhesion molecule upregulation in cultured human endothelial cells: role of nuclear factor-κB. The J. Nutr., 134(5): 1013-1019.

Cushnie, T.P., Lamb, A.J., 2005. Antimicrobial activity of flavonoids. Int. J. Antimicrob. Agents, 26(5): 343-56.

De Jong, W.H., Borm, P.J.A., 2008. Drug delivery and nanoparticles:applications and hazards. Int. J. Nanomed., 3(2): 133-149.

El-Hashash, M.A., Darwish, K.M., Rizk, S.A., El-Bassiouny, F.A., 2011. The uses of 2-ethoxy-(4H)-3, 1-benzoxazin-4-one in the synthesis of some quinazolinone derivatives of antimicrobial activity. Pharm., 4(7): 1032-1051.

El-Hashash, M.A., Rizk, S.A., Atta-Allah, S.R., 2015. Synthesis and regioselective reaction of some unsymmetrical heterocyclic chalcone derivatives and spiro heterocyclic compounds as antibacterial agents. Molec., 20(12): 22069-22083.

El-Hashash, M.A., Rizk, S.A., 2017. One-pot Synthesis of Novel Spirooxindoles as Antibacterial and Antioxidant Agents. J. Heterocycl. Chem., 54(3): 1776-1784.

Elkholy, A.E., Rizk, S.A., Rashad, A.M., 2019. Enhancing lubricating oil properties using novel quinazolinone derivatives: DFT study and molecular dynamics simulation. J. Mol. Struct., 1175: 788-796.

Erlund, I., 2004. Review of the flavonoids quercetin, hesperetin, and naringenin. Dietary sources, bioactivities, bioavailability, and epidemiology. Nutr. Res., 24(10): 851-874.

Gattuso, G., Barreca, D., Gargiulli, C., Leuzzi, U., Caristi, C., 2007. Flavonoid composition of citrus juices. Molec., 12(8): 1641-1673.

Gattuso, G. et al., 2006. Flavonoid glycosides in bergamot juice (*Citrus bergamia* Risso). J. Agric. Food Chem., 54(11): 3929-3935.

Gil-Izquierdo, A., Gil, M.I., Ferreres, F., 2002. Effect of processing techniques at industrial scale on orange juice antioxidant and beneficial health compounds. J. Agric. Food Chem., 50(18): 5107-5114.

Gil-Izquierdo, A., Riquelme, M.T., Porras, I., Ferreres, F., 2004. Effect of the rootstock and interstock grafted in lemon tree (*Citrus limon* (L.) Burm.) on the flavonoid content of lemon juice. J. Agric. Food Chem., 52(2): 324-31.

Gross, M., 2004. Flavonoids and Cardiovascular Disease. Pharm. Biol., 42(sup1): 21-35.

Hara, H. et al., 2011. Inhibitory effects of chalcone glycosides isolated from Brassica rapa L. 'hidabeni' and their synthetic derivatives on LPS-induced NO production in microglia. Bioorg. Med. Chem., 19(18): 5559-68.

Heakal, F.E.-T., Attia, S., Rizk, S., Abou Essa, M., Elkholy, A., 2017. Synthesis, characterization and computational chemical study of novel pyrazole derivatives as anticorrosion and antiscalant agents. J. Mol. Struct., 1147: 714-724.

Hirano, R. et al., 2001. Antioxidant ability of various flavonoids against DPPH radicals and LDL oxidation. J. Nutr. Sci. Vitaminol., 47(5): 357-362.

Hussain, F. et al., 2016. Antibacterial Activities of Methanolic Extracts of Datura inoxia. PSM Microbiol., 1(1): 33-35.

Hussein, M.A. et al., 2018. Synthesis, molecular docking and insecticidal activity evaluation of chromones of date palm pits extract against *Culex pipiens* (Diptera: Culicidae). Int. J. Mosq. Res, 5(4): 22-32.

Iqbal, M.N., Ashraf, A., 2019. *Withania somnifera*: Can it be a Therapeutic Alternative for Microbial Diseases in an Era of Progressive Antibiotic Resistance? Int. J. Nanotechnol. Allied Sci., 3(1): 16-18.

Jaddoa, K., Ibrahim, B., 2014. Role of yeast extract in the growth of black seed callus and production of secondary metabolism compounds. Iraqi J. Agric. Sci., 45(7): 685-691.

Kalim, M., Hussain, F., Ali, H., Ahmad, I., Iqbal, M.N., 2016. Antifungal Activities of Methanolic Extracts of *Datura inoxia*. PSM Biol. Res., 1(2): 70-73.

Kim, H.P., Son, K.H., Chang, H.W., Kang, S.S., 2004. Anti-inflammatory plant flavonoids and cellular action mechanisms. J. Pharmacol. Sci., 96(3): 229-45.

Knekt, P. et al., 2002. Flavonoid intake and risk of chronic diseases. The Am. J. Clin. Nutr., 76(3): 560-568.

Kris-Etherton, P.M. et al., 2004. Bioactive compounds in nutrition and health-research methodologies for establishing biological function: the antioxidant and anti-inflammatory effects of flavonoids on atherosclerosis. Annu. Rev. Nutr., 24: 511-538.

Lotito, S.B., Frei, B., 2006. Dietary flavonoids attenuate tumor necrosis factor α-induced adhesion molecule expression in human aortic endothelial cells: structure-function relationships and activity after first pass metabolism. J. Biol. Chem., 281(48): 37102-37110.

Materska, M., Perucka, I., 2005. Antioxidant activity of the main phenolic compounds isolated from hot pepper fruit (Capsicum annuum L). J. Agric. Food Chem., 53(5): 1750-6.

Meignanalakshmi, S., Vinoth Kumar, S., Deepika, J., Farida Begum, I., 2013. Evaluation of antibacterial activity of methanol extract of leaves of *Adhatoda vasica* on mastitis pathogens. Hygela J. Drugs Med., 5: 1-4.

Middleton, E., Jr., Kandaswami, C., 1992. Effects of flavonoids on immune and inflammatory cell functions. Biochem. Pharmacol., 43(6): 1167-79.

Minato, K. et al., 2003. Lemon flavonoid, eriocitrin, suppresses exercise-induced oxidative damage in rat liver. Life Sci., 72(14): 1609-16.

Miyake, Y., 2006. Characteristics of Flavonoids in Niihime Fruit-a New Sour Citrus Fruit. Food Sci. Technol. Res., 12: 186-193.

Miyake, Y., Yamamoto, K., Morimitsu, Y., Osawa, T., 1997. Isolation of C-glucosylflavone from lemon peel and antioxidative activity of flavonoid compounds in lemon fruit. J. Agric. Food Chem., 45(12): 4619-4623.

Nichenametla, S.N., Taruscio, T.G., Barney, D.L., Exon, J.H., 2006. A review of the effects and mechanisms of polyphenolics in cancer. Crit. Rev. Food Sci. Nutr., 46(2): 161-83.

Nijveldt, R.J. et al., 2001. Flavonoids: a review of probable mechanisms of action and potential applications. Am. J. Clin. Nutr., 74(4): 418-25.

Nogata, Y. et al., 2006. Flavonoid composition of fruit tissues of citrus species. Biosci., Biotechnol., Biochem., 70(1): 178-192.

Oyama, K.-i., Kondo, T., 2004. Total synthesis of apigenin 7, 4′-di-O-β-glucopyranoside, a component of blue flower pigment of Salvia patens, and seven chiral analogues. Tetrahedron., 60(9): 2025-2034.

Pauli, G.F., Junior, P., 1995. Phenolic glycosides from *Adonis aleppica*. Phytochem., 38(5): 1245-1250.

Pretto, F.R., Santarém, E.R., 2000. Callus formation and plant regeneration from Hypericum perforatum leaves. Plant Cell Tissue Organ Cult., 62(2): 107-113.

Rabie, K.A., El-Aal, A., Mona, S., Manaf, H., 2010. Enhanced silymarin accumulation as influence of medium composition in cell suspension cultures of *Silybum marianum* (l.) gaertn. J. Plant Produc., 1(2): 319-332.

Rizk, S.A., Abdelwahab, S.S., Elrazaz, E., 2019. Synthesis and QSAR study of some novel heterocyclic derivatives as in vitro cytotoxic agents. J. Heterocycl. Chem., 56(2): 443-449.

Rizk, S.A., El-Naggar, A.M., El-Badawy, A.A., 2018a. Synthesis, spectroscopic characterization and computational chemical study of 5-cyano-2-thiouracil derivatives as potential antimicrobial agents. J. Mol. Struct., 1155: 720-733.

Rizk, S.A., El-Hashash, M.A., El-Badawy, A.A., 2017. Ultrasonic and Grinding Aptitudes of One-Pot Synthesis of 5-(4-Chlorophenyl)-7-(3, 4-Dimethyl Phenyl)-2-oxo-2H-Pyrano [2, 3-b] Pyridine Derivatives as Antibacterial Agents. J. Heterocycl. Chem., 54(3): 2003-2011.

Rizk, S.A., Elsayed, G.A., El-Hashash, M.A., 2018b. One-pot synthesis, spectroscopic characterization and DFT study of novel 8-azacoumarin derivatives as eco-friendly insecticidal agents. J. Iran. Chem. Soc., 15(9): 2093-2105.

Sánchez-Moreno, C., Plaza, L., de Ancos, B., Cano, M.P., 2003. Quantitative bioactive compounds assessment and their relative contribution to the antioxidant capacity of commercial orange juices. J. Sci. Food and Agric., 83(5): 430-439.

Scalbert, A., Manach, C., Morand, C., Rémésy, C., Jiménez, L., 2005. Dietary polyphenols and the prevention of diseases. Crit. Rev. Food Sci. Nutr., 45(4): 287-306.

Shimoi, K., Saka, N., Kaji, K., Nozawa, R., Kinae, N., 2000. Metabolic fate of luteolin and its functional activity at focal site. BioFactors, 12(1-4): 181-6.

Steinberg, D., 1989. Modifications of low-density lipoprotein that increase its atherogenicity. N. Engl. J. Med., 320: 915-924.

Takaya, Y., Kondo, Y., Furukawa, T., Niwa, M., 2003. Antioxidant constituents of radish sprout (Kaiware-daikon), *Raphanus sativus* L. J. Agric. Food Chem., 51(27): 8061-6.

Tijburg, L.B., Mattern, T., Folts, J.D., Weisgerber, U.M., Katan, M.B., 1997. Tea flavonoids and cardiovascular disease: a review. Crit. Rev. Food Sci. Nutr., 37(8): 771-85.

Walker, T.S., Bais, H.P., Vivanco, J.M., 2002. Jasmonic acid-induced hypericin production in cell suspension cultures of *Hypericum perforatum* L.(St. John's wort). Phytochem., 60(3): 289-293.

Wightman, J.D., 2003. Red Berries and Their Health Benefits, Nutraceutical Beverages. ACS Symposium Series. Am. Chem. Soc., pp. 123-132.

Xi, Q., Lai, W., Cui, Y., Wu, H., Zhao, T., 2019. Effect of yeast extract on seedling growth promotion and soil improvement in afforestation in a semiarid chestnut soil area. Forests, 10(1): 76.